Available online at www.sciencedirect.com
SCIENCE DIRECT®
Mechanical Systems and Signal Processing 18 (2004) 1–27
Mechanical Systems and Signal Processing
www.elsevier.com/locate/jnlabr/ymssp

Optimal complex modes and an index of damping non-proportionality

S. Adhikari*,[1]

Department of Engineering, University of Cambridge, Trumpington Street, Cambridge CB2 1PZ, UK

Received 19 September 2000; received in revised form 21 June 2001; accepted 4 July 2001

Abstract

In general, damped linear systems possess complex modes instead of classical normal modes. In this paper, complex modes arising due to non-proportionality of the damping are considered. A simple method is proposed to normalise the complex modes so that they are closest to their corresponding classical normal modes. Based on these 'optimal complex modes', an index of damping non-proportionality is proposed. The methodologies developed here are applicable to both viscous and non-viscously damped systems. Numerical examples are provided to illustrate the developed concepts.

1. Introduction

The equations of motion describing the free vibration of an undamped linear system with N degrees of freedom (dof's) can be expressed by

$$\mathbf{M}\ddot{\mathbf{q}}(t) + \mathbf{K}\mathbf{q}(t) = \mathbf{0}. \tag{1.1}$$

In the above equation, the real symmetric matrices $\mathbf{M} \in \mathbb{R}^{N\times N}$ and $\mathbf{K} \in \mathbb{R}^{N\times N}$ are known as the mass and stiffness matrices, respectively, and $\mathbf{q}(t) \in \mathbb{R}^N$ is the vector of the generalised coordinates. Rayleigh [1] has shown that undamped linear systems, equations of motion of which are given by Eq. (1.1), are capable of so-called *natural motions*. This essentially implies that all the system coordinates execute harmonic oscillation at a given frequency and form a certain displacement pattern. The oscillation frequency and displacement pattern are called *natural frequencies* (ω_j) and *normal modes* ($\mathbf{x}_j$), respectively. Using the normal modes it is possible to decouple the equations of

*Fax: +44-1223-332662.
E-mail address: sa225@eng.cam.ac.uk (S. Adhikari).
[1] Member, Trinity College, Cambridge.

0888-3270/04/$ - see front matter
doi:10.1016/S0888-3270(03)00048-7

motion (1.1), that is, if $\mathbf{X} = [\mathbf{x}_1, \mathbf{x}_2, \ldots, \mathbf{x}_N] \in \mathbb{R}^{N\times N}$ is the modal matrix, then $\mathbf{X}^T\mathbf{M}\mathbf{X}$ and $\mathbf{X}^T\mathbf{K}\mathbf{X}$ are diagonal matrices.

These simple facts in general do not hold for damped systems. For viscously damped systems, if the viscous damping matrix $\mathbf{C}$ has the form

$$\mathbf{C} = \alpha_m\mathbf{M} + \alpha_k\mathbf{K}, \quad \alpha_m, \alpha_k \in \mathbb{R} \tag{1.2}$$

then the equations of motion of damped systems can be diagonalised using the undamped modal matrix $\mathbf{X}$. This damping model is known as proportional damping or classical damping. Caughey and O'Kelly [2] have shown that such diagonalisation is possible if and only if $\mathbf{K}\mathbf{M}^{-1}\mathbf{C} = \mathbf{C}\mathbf{M}^{-1}\mathbf{K}$. In general, linear systems do not satisfy this condition and consequently they do not possess classical normal modes but possess *complex modes*. Complex modes, however, can arise for various other reasons [3], for example, due to the gyroscopic effects, aerodynamic effects, non-linearity and experimental noise. In this paper, we discuss complex modes that arise only due to the non-proportional nature of the damping.

There exists extensive literature on viscously damped systems with non-proportional damping. Due to the non-proportional nature of the damping, the equations of motion are coupled through the modal damping matrix, $\mathbf{C}' = \mathbf{X}^T\mathbf{C}\mathbf{X}$. A common approach in this case is simply to ignore the off-diagonal terms of the modal damping matrix $\mathbf{C}'$ which couple the equations of motion. This approach is known as approximate decoupling method. For large-scale systems, the computational effort in adopting the decoupling approximation is an order of magnitude smaller than the methods of complex modes. Several authors, for example [4–17], have investigated the effects of decoupling approximation. Some general conclusions arising from these studies are that the solution of the decoupled equation would be close to the exact solution of the coupled equations if $\mathbf{C}'$ is a diagonally dominant matrix and undamped natural frequencies are adequately separated. Motivated by these results, several authors have proposed numerical indices to quantify the degree of non-proportionality of the damping (will be discussed in Section 5).

All the above studies explicitly or implicitly assume that the damping is viscous. In this paper, these studies are extended to non-viscously damped systems. Possibly, the most general way to model damping within the linear range is to use non-viscous damping models which depend on the past history of motion via convolution integrals over some kernel functions. The damping force using such a model can be expressed by

$$\mathbf{F}_d(t) = \int_{-\infty}^{t} \mathscr{G}(t-\tau)\dot{\mathbf{q}}(\tau)\,\mathrm{d}\tau. \tag{1.3}$$

The kernel functions $\mathscr{G}(t) \in \mathbb{R}^{N\times N}$, or others closely related to them, are described under many different names in the literature of different subjects: for example, retardation functions, heredity functions, after-effect functions, relaxation functions, etc. This model was originally introduced by Biot [18]. In the special case when $\mathscr{G}(t-\tau) = \mathbf{C}\delta(t-\tau)$, Eq. (1.3) reduces to the case of viscous damping. The damping model of this kind is a further generalisation of the familiar viscous damping. Recently, Adhikari [19] has shown that existence of normal modes in linear systems with such damping is possible if and only if any one of the following conditions is

satisfied:

$$\mathbf{K}\mathbf{M}^{-1}\mathscr{G}(t) = \mathscr{G}(t)\mathbf{M}^{-1}\mathbf{K} \tag{1.4a}$$

$$\mathbf{M}\mathbf{K}^{-1}\mathscr{G}(t) = \mathscr{G}(t)\mathbf{K}^{-1}\mathbf{M} \tag{1.4b}$$

$$\mathbf{M}\mathscr{G}^{-1}(t)\mathbf{K} = \mathbf{K}\mathscr{G}^{-1}(t)\mathbf{M}. \tag{1.4c}$$

From this result it follows that, like viscously damped systems, complex modes can arise in non-viscously damped systems when the damping is non-proportional. Practical experience in modal testing also shows that most real-life structures possess complex modes instead of real normal modes. However, in spite of a large amount of research, understanding of complex modes is not well developed as real normal modes. A major reason for this is that, by contrast with real normal modes, the 'shapes' of complex modes are not in general clear. Moreover, it appears that unlike the (real) scaling of real normal modes, the (complex) scaling or normalisation of complex modes has a significant effect on their geometric appearance. Since the real normal modes are well understood, in this paper a method is presented to normalise the complex modes such that they are closest (according to some definition of 'closeness') to their corresponding normal modes. Such complex modes will be called *optimally normalised complex modes* or simply *optimal complex modes*. The motivation for seeking the optimal complex modes arises from the following facts:

- to view complex modes as an extension of our existing knowledge of real normal modes;
- to understand the shapes of the real and imaginary parts of a complex mode when it is closest to its corresponding real normal mode;
- to quantify the amount of 'complexity' of a measured complex mode from the difference between the optimal complex mode and the corresponding real normal mode.

In Sections 2 and 3, complex modes in viscously and non-viscously damped systems are briefly discussed. In Section 4, a method is proposed to normalise the complex modes such that they are closest to their corresponding normal modes. Since only the geometric properties of the complex modes are utilised, the method is independent of the nature of the damping (i.e. viscous or non-viscous) of the system. Based on this optimally normalised complex modes, in Section 5, an index is developed to quantify the extent of non-proportionality of damping. In Section 6, a different approach to normalise complex modes based on weighted sums of the real and imaginary parts is presented. Applications of the optimal complex modes and the newly developed index of non-proportionality are illustrated through numerical examples on viscously and non-viscously damped systems. Finally, Section 7 summarises the main findings of this paper.

2. Complex modes in viscously damped systems

The equations of motion describing free vibration of a viscously damped linear discrete system with N dof's can be written as

$$\mathbf{M}\ddot{\mathbf{q}}(t) + \mathbf{C}\dot{\mathbf{q}}(t) + \mathbf{K}\mathbf{q}(t) = \mathbf{0}. \tag{2.1}$$

The eigenvalue problem associated with Eq. (2.1) can be represented by

$$s_k^2\mathbf{M}\mathbf{z}_k + s_k\mathbf{C}\mathbf{z}_k + \mathbf{K}\mathbf{z}_k = \mathbf{0} \tag{2.2}$$

where $s_k \in \mathbb{C}$ is the kth eigenvalue and $\mathbf{z}_k \in \mathbb{C}^N$ is the kth eigenvector. The eigenvalues, s_k, are the roots of the characteristic polynomial

$$\det[s^2\mathbf{M} + s\mathbf{C} + \mathbf{K}] = 0. \tag{2.3}$$

The order of the polynomial is $2N$ and if the roots are complex they appear in complex conjugate pairs. Several authors, [20,21] for example, have studied non-classically damped linear systems using the state-space methods. Following the state-space approach it may be shown [22] that each complex mode satisfies the normalisation relationship

$$\mathbf{z}_k^T[2s_k\mathbf{M} + \mathbf{C}]\mathbf{z}_k = \theta_k, \quad \forall k = 1, \ldots, 2N \tag{2.4}$$

for some non-zero $\theta_k \in \mathbb{C}$. Numerical values of θ_k can be selected in various ways:

(a) Choose [23]

$$\theta_k = 2s_k, \quad \forall k. \tag{2.5a}$$

This reduces to $\mathbf{z}_k^T\mathbf{M}\mathbf{z}_k = 1, \forall k$ when the damping is zero, which is consistent with the unity modal-mass convention, often used in experimental modal analysis and finite element (FE) methods.

(b) Choose [22]

$$\theta_k = 2\mathrm{i}\Im(s_k), \quad \forall k. \tag{2.5b}$$

Like the previous normalisation this also reduces to the unity modal-mass convention when the damping is zero. In Ref. [22], it was mentioned (without proof) that the imaginary parts of the modes are minimised and the real parts are maximised with this normalisation.

(c) Choose [23,22]

$$\theta_k = 1 + \mathrm{i}0, \quad \forall k. \tag{2.5c}$$

Theoretical analysis becomes easiest with this normalisation. However, as pointed out in [23,24], this normalisation is inconsistent with undamped or classically damped modal theories.

It should be noted that normalisation of complex modes according to the above choices does not render them to be closest to the corresponding undamped modes. This issue will be discussed further in Section 4.

3. Complex modes in non-viscously damped systems

The equations of motion describing free vibration of an N-dof linear system with non-viscous damping of the form (1.3) can be expressed by

$$\mathbf{M}\ddot{\mathbf{q}}(t) + \int_0^t \mathscr{G}(t-\tau)\dot{\mathbf{q}}(\tau)\,\mathrm{d}\tau + \mathbf{K}\mathbf{q}(t) = \mathbf{0}. \tag{3.1}$$

The eigenvalue problem associated with this equation can be defined by taking the Laplace transform as

$$s_k^2\mathbf{M}\mathbf{z}_k + s_k\mathbf{G}(s_k)\mathbf{z}_k + \mathbf{K}\mathbf{z}_k = \mathbf{0} \tag{3.2}$$

where $\mathbf{G}(s)$ is the Laplace transform of $\mathscr{G}(t)$. The eigenvalue problem of the form (3.2) has been discussed by Adhikari [25]. Here we briefly outline the main features.

The eigenvalues, s_k, associated with Eq. (3.2) are roots of the characteristic equation

$$\det[s^2\mathbf{M} + s\mathbf{G}(s) + \mathbf{K}] = 0. \tag{3.3}$$

For the linear viscoelastic case, it can be shown that [26,27], in general, the elements of $\mathbf{G}(s)$ can be represented by

$$G_{jk}(s) = \frac{p_{jk}(s)}{q_{jk}(s)} \tag{3.4}$$

where $p_{jk}(s)$ and $q_{jk}(s)$ are finite-order polynomials in s and the degree of $p_{jk}(s)$ is not more than that of $q_{jk}(s)$. Under such assumptions, it is easy to see that the order of the characteristic equation, m, is more than $2N$, that is $m = 2N + p; p \geqslant 0$. Thus, although the system has N dof's, the number of eigenvalues is more than $2N$. This is a major difference between non-viscously damped systems and viscously damped systems where the number of eigenvalues is exactly $2N$, including any multiplicities. Following Adhikari [25], one may group the eigenvectors as (a) elastic modes (corresponding to N complex conjugate pairs of eigenvalues), and (b) non-viscous modes (corresponding to the 'additional' p eigenvalues). The elastic modes are related to the N modes of vibration of structural systems and the non-proportional nature of the damping affects only the elastic modes. Thus, in this paper we will discuss the elastic modes only.

Following Adhikari [28], the normalisation relationship satisfied by the modes of non-viscously damped systems may be expressed as

$$\mathbf{z}_k^T\left[2s_k\mathbf{M} + \mathbf{G}(s_k) + s_k\frac{\partial[\mathbf{G}(s)]}{\partial s}|s_k\right]\mathbf{z}_k = \theta_k, \quad \forall k = 1, \ldots, m. \tag{3.5}$$

Note that Eq. (3.5) reduces to Eq. (2.4), the corresponding relationship for viscously damped systems, when $\mathbf{G}(s)$ is constant with respect to s. For non-viscously damped systems one can also select θ_k following Eqs. (2.5a)–(2.5c).

4. Optimal normalisation of complex modes

4.1. Theory

Normalisation of complex modes still remains an issue to be addressed. We know that normalisation of real modes using real constants is a simple 'scaling' of the mode shapes. This simple fact in general does not hold for complex modes. Normalisation of complex modes using complex constants deforms the 'shape' of the modes because relative values of the real and imaginary parts change. For this reason, unlike real modes, the geometric appearance of complex modes depends on the normalisation procedure. Here we consider how to normalise complex modes so that they are closest in a least-square sense to their corresponding normal modes. Such

complex modes are called *optimally normalised complex modes* or simply *optimal complex modes*. Next, a simple least-square error minimisation approach is presented to obtain optimal complex modes.

Consider that $\hat{\mathbf{z}}_j \in \mathbb{C}^N$ is the jth complex mode obtained from modal testing and N denotes the number of measurement points on the structure. Suppose that the number of modes to be considered in the study is n: in general $n \neq N$, usually $N \geqslant n$. Assume that the mass-normalised normal modes $\mathbf{x}_j \in \mathbb{R}^N$, $\forall j = 1, \ldots, n$, satisfying

$$\mathbf{x}_j^T \mathbf{M} \mathbf{x}_j = 1, \quad \forall j = 1, \ldots, n \tag{4.1}$$

are known. Consider that the optimal complex modes, $\mathbf{z}_j$, are related with the measured complex modes through

$$\mathbf{z}_j = \hat{\mathbf{z}}_j \lambda_j \tag{4.2}$$

for some non-zero $\lambda_j \in \mathbb{C}$. Separating the real and imaginary parts of $\hat{\mathbf{z}}_j$ and λ_j, we write

$$\hat{\mathbf{z}}_j = \hat{\mathbf{u}}_j + \mathrm{i}\hat{\mathbf{v}}_j \tag{4.3}$$

and

$$\lambda_j = \alpha_j + \mathrm{i}\beta_j \tag{4.4}$$

where $\hat{\mathbf{u}}_j, \hat{\mathbf{v}}_j \in \mathbb{R}^N$ and $\alpha_j, \beta_j \in \mathbb{R}$. Using Eqs. (4.3) and (4.4), Eq. (4.2) can be written as

$$\mathbf{z}_j = (\hat{\mathbf{u}}_j \alpha_j - \hat{\mathbf{v}}_j \beta_j) + \mathrm{i}(\hat{\mathbf{v}}_j \alpha_j + \hat{\mathbf{u}}_j \beta_j). \tag{4.5}$$

Denote the difference between $\mathbf{z}_j$ and $\mathbf{x}_j$,

$$\varepsilon_j = \mathbf{x}_j - \mathbf{z}_j \in \mathbb{C}^N. \tag{4.6}$$

It is required to find α_j and β_j such that the norm of ε_j (in some sense) is minimised. In this paper, we consider the Euclidean norm or l_2 norm in $\mathbb{R}^N$. Because ε_j is complex, it is required to consider the real and imaginary parts separately. Write

$$\varepsilon_j = \varepsilon_{R_j} + \mathrm{i}\varepsilon_{I_j} \tag{4.7}$$

where, due to Eq. (4.5),

$$\varepsilon_{R_j} = \mathbf{x}_j - \hat{\mathbf{u}}_j \alpha_j + \hat{\mathbf{v}}_j \beta_j \tag{4.8}$$

and

$$\varepsilon_{I_j} = -(\hat{\mathbf{v}}_j \alpha_j + \hat{\mathbf{u}}_j \beta_j). \tag{4.9}$$

In order to minimise the Euclidean norm of the real and imaginary parts of $\varepsilon_j, \forall j = 1, \ldots, n$, define two *merit functions*

$$\chi_R^2 = \sum_{j=1}^{n} \varepsilon_{R_j}^T \varepsilon_{R_j} \tag{4.10}$$

and

$$\chi_I^2 = \sum_{j=1}^{n} \varepsilon_{I_j}^T \varepsilon_{I_j}. \tag{4.11}$$

Consider χ_R^2 first. To obtain α_k and β_k such that χ_R^2 is minimised, set

$$\frac{\partial \chi_R^2}{\partial \alpha_k} = 0, \quad \forall k = 1, \ldots, n \tag{4.12}$$

and

$$\frac{\partial \chi_R^2}{\partial \beta_k} = 0, \quad \forall k = 1, \ldots, n. \tag{4.13}$$

Substituting ε_{R_j} from Eq. (4.8), Eq. (4.12) gives

$$2(-\hat{\mathbf{u}}_k^T)(\mathbf{x}_k - \hat{\mathbf{u}}_k\alpha_k + \hat{\mathbf{v}}_k\beta_k) = 0 \tag{4.14}$$

or

$$(\hat{\mathbf{u}}_k^T\hat{\mathbf{u}}_k)\alpha_k - (\hat{\mathbf{u}}_k^T\hat{\mathbf{v}}_k)\beta_k = (\hat{\mathbf{u}}_k^T\mathbf{x}_k).$$

Similarly, from Eq. (4.13) one obtains

$$-(\hat{\mathbf{v}}_k^T\hat{\mathbf{u}}_k)\alpha_k + (\hat{\mathbf{v}}_k^T\hat{\mathbf{v}}_k)\beta_k = -(\hat{\mathbf{v}}_k^T\mathbf{x}_k). \tag{4.15}$$

Again, considering χ_I^2, substituting ε_{I_j} from Eq. (4.9) and differentiating with respect to α_k and β_k we obtain

$$(\hat{\mathbf{v}}_k^T\hat{\mathbf{v}}_k)\alpha_k + (\hat{\mathbf{v}}_k^T\hat{\mathbf{u}}_k)\beta_k = 0 \tag{4.16}$$

and

$$(\hat{\mathbf{u}}_k^T\hat{\mathbf{v}}_k)\alpha_k + (\hat{\mathbf{u}}_k^T\hat{\mathbf{u}}_k)\beta_k = 0. \tag{4.17}$$

Now define a new merit function χ^2 as the sum of χ_R^2 and χ_I^2 to consider the real and imaginary parts together, that is, define

$$\chi^2 = \chi_R^2 + \chi_I^2. \tag{4.18}$$

Using this definition of χ^2, Eqs. (4.14)–(4.17) can be combined into two equations and may be expressed in a matrix form as

$$\begin{bmatrix} (\hat{\mathbf{u}}_k^T\hat{\mathbf{u}}_k) + (\hat{\mathbf{v}}_k^T\hat{\mathbf{v}}_k) & 0 \\ 0 & (\hat{\mathbf{v}}_k^T\hat{\mathbf{v}}_k) + \hat{\mathbf{u}}_k^T\hat{\mathbf{u}}_k) \end{bmatrix} \begin{Bmatrix} \alpha_k \\ \beta_k \end{Bmatrix} = \begin{Bmatrix} (\hat{\mathbf{u}}_k^T\mathbf{x}_k) \\ -(\hat{\mathbf{v}}_k^T\mathbf{x}_k) \end{Bmatrix}. \tag{4.19}$$

In the above equation, we have used $\hat{\mathbf{v}}_k^T\hat{\mathbf{u}}_k = \hat{\mathbf{u}}_k^T\hat{\mathbf{v}}_k$. Also note that $\hat{\mathbf{u}}_k^T\hat{\mathbf{u}}_k = \|\hat{\mathbf{u}}_k\|^2$ and $\hat{\mathbf{v}}_k^T\hat{\mathbf{v}}_k = \|\hat{\mathbf{v}}_k\|^2$. Solving Eq. (4.19), α_k and β_k can be obtained for every k as

$$\alpha_k = \frac{\hat{\mathbf{u}}_k^T\mathbf{x}_k}{\|\hat{\mathbf{u}}_k\|^2 + \|\hat{\mathbf{v}}_k\|^2} \quad \text{and} \quad \beta_k = -\frac{\hat{\mathbf{v}}_k^T\mathbf{x}_k}{\|\hat{\mathbf{u}}_k\|^2 + \|\hat{\mathbf{v}}_k\|^2}. \tag{4.20}$$

A more general case when χ^2 is expressed as the weighted sum of χ_R^2 and χ_I^2 is discussed in Section 6.

A geometric interpretation of the normalisation constants α_k and β_k expressed in Eq. (4.20) is useful. The numerator of the expression for α_k is the projection of the vector $\hat{\mathbf{u}}_k$ along $\mathbf{x}_k$ in $\mathbb{R}^N$ while the denominator is the sum of the lengths (squared) of $\hat{\mathbf{u}}_k$ and $\hat{\mathbf{v}}_k$. Similarly, the imaginary parts of the normalisation constants are associated with the projection of the imaginary parts of the measured complex modes along $\mathbf{x}_k$. Substituting the expressions for α_k and β_k from Eq. (4.20)

into Eq. (4.5), the *optimal complex modes* can be obtained as

$$\mathbf{z}_k = \frac{\hat{\mathbf{u}}_k(\hat{\mathbf{u}}_k^T\mathbf{x}_k) + \hat{\mathbf{v}}_k(\hat{\mathbf{v}}_k^T\mathbf{x}_k)}{\|\hat{\mathbf{u}}_k\|^2 + \|\hat{\mathbf{v}}_k\|^2} + \mathrm{i}\frac{\hat{\mathbf{v}}_k(\hat{\mathbf{u}}_k^T\mathbf{x}_k) - \hat{\mathbf{u}}_k(\hat{\mathbf{v}}_k^T\mathbf{x}_k)}{\|\hat{\mathbf{u}}_k\|^2 + \|\hat{\mathbf{v}}_k\|^2}. \tag{4.21}$$

Note that only the measured complex modes and normal modes are required in order to evaluate Eq. (4.21). For this reason, neither the mass and stiffness matrices, nor the damping matrix (viscous or non-viscous) are required to obtain the optimally normalised complex mode. This fact makes this approach particularly useful compared to the conventional normalisation relationships (Eqs. (2.4) and (3.5)) which require knowledge of the system property matrices.

4.2. Numerical examples

4.2.1. A two-dof system

Consider a viscously damped two-dof system shown in Fig. 1 with numerical values assumed for the system parameters. The complex eigenvalues of the system corresponding to the two modes are $s_1 = -1.3786 \pm 32.5838\mathrm{i}$ and $s_2 = -2.6214 \pm 33.5570\mathrm{i}$. Q-factors (defined as $Q_j = \Im(s_j)/2\Re(s_j)$) for the two modes, $Q_1 = 11.8178$ and $Q_2 = 6.4006$, indicate that the damping is quite high for both the modes. The mass-normalised normal modes of the system, i.e. the eigenvectors without damping, are obtained as

$$\mathbf{x}_1 = \begin{Bmatrix} 0.9239 \\ 0.3827 \end{Bmatrix} \quad \text{and} \quad \mathbf{x}_2 = \begin{Bmatrix} -0.3827 \\ 0.9239 \end{Bmatrix}. \tag{4.22}$$

The complex modes, normalised according to Eq. (2.4) with $\theta_k = 2s_k$, are

$$\hat{\mathbf{z}}_1 = \begin{Bmatrix} 0.8463 - 0.3349\mathrm{i} \\ 0.7538 + 0.3877\mathrm{i} \end{Bmatrix} = \hat{\mathbf{u}}_1 + \mathrm{i}\hat{\mathbf{v}}_1 \quad \text{and} \quad \hat{\mathbf{z}}_2 = \begin{Bmatrix} -0.7589 - 0.4241\mathrm{i} \\ 0.8296 - 0.3259\mathrm{i} \end{Bmatrix} = \hat{\mathbf{u}}_2 + \mathrm{i}\hat{\mathbf{v}}_2. \tag{4.23}$$

In a two-dimensional (2-D) space ($\mathbb{R}^2$) each vector, $\mathbf{x}_k$, $\hat{\mathbf{u}}_k$, and $\hat{\mathbf{v}}_k$, represents a 'point'. Plots of these vectors for the two modes considering the origin at (0,0) are shown in Figs. 2 and 3. The optimal complex modes for the system, obtained by applying Eq. (4.21), are

$$\mathbf{z}_1 = \begin{Bmatrix} 0.6205 - 0.1436\mathrm{i} \\ 0.4812 + 0.3467\mathrm{i} \end{Bmatrix} = \mathbf{u}_1 + \mathrm{i}\mathbf{v}_1 \quad \text{and} \quad \mathbf{z}_2 = \begin{Bmatrix} -0.4794 - 0.3571\mathrm{i} \\ 0.5948 - 0.1479\mathrm{i} \end{Bmatrix} = \mathbf{u}_2 + \mathrm{i}\mathbf{v}_2. \tag{4.24}$$

In Figs. 2 and 3, $\mathbf{u}_k$ and $\mathbf{v}_k$ are also plotted. From these figures, one can observe how the proposed optimal normalisation procedure brings the complex modes closer to the normal modes.

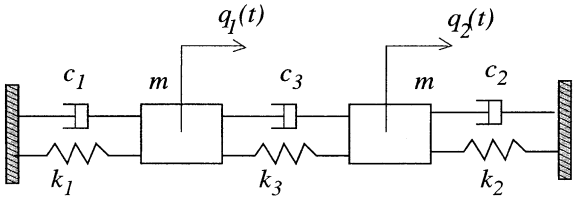

Fig. 1. A two-dof system with non-proportional damping: $m = 1$ kg, $k_1 = 1000$ N/m, $k_2 = 1100$ N/m, $k_3 = 50$ N/m, $c_1 = 3.0$ N s/m, $c_2 = 1.0$ N s/m, $c_3 = 2.0$ N s/m.

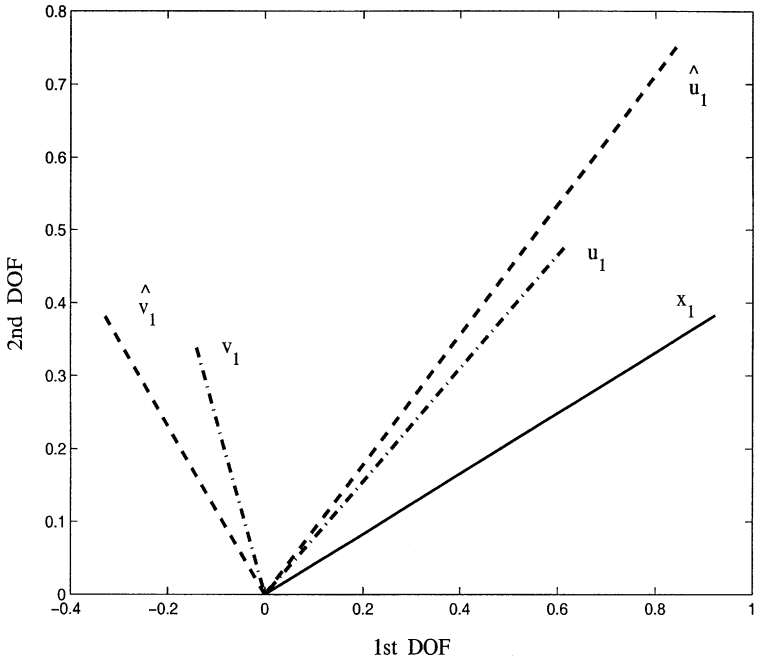

Fig. 2. Graphical (vector) representation of the real and imaginary parts of the first complex mode: 'O' origin; '–' normal mode $\mathbf{x}_1$; '- -' real and imaginary parts of the complex mode $\hat{\mathbf{z}}_1$ normalised using Eq. (2.4) with $\theta_1 = 2s_1$; '-.-' real and imaginary parts of the optimally normalised complex mode $\mathbf{z}_1$ obtained from Eq. (4.21).

Unfortunately, this graphical representation procedure of the complex modes cannot be extended to more than three dof systems. For this reason a different and more general approach is presented in the next example.

4.2.2. A 10-dof system

A system consisting of a linear array of spring–mass oscillators and dampers is considered to illustrate the optimal complex modes. Fig. 4 shows the model system. N masses, each of nominal mass m_u, are connected by springs of nominal stiffness k_u. The mass matrix of the system has the form $\mathbf{M} = m_u\mathbf{I}_N$, where $\mathbf{I}_N$ is the $N \times N$ identity matrix. The stiffness matrix of the system is

$$\mathbf{K} = k_u \begin{bmatrix} 2 & -1 & & & & & & & & \\ -1 & 2 & -1 & & & & & & & \\ & \ddots & \ddots & \ddots & & & & & & \\ & & -1 & 2 & -1 & & & & & \\ & & & \ddots & \ddots & -1 & & & & \\ & & & & -1 & 2 & & & & \end{bmatrix}. \tag{4.25}$$

Some of the masses of the system shown in Fig. 4 have viscous dampers connecting them to the ground. The damping matrix can be expressed as $\mathbf{C} = c_u\bar{\mathbf{I}}$, where c_u is the viscous damping constant and $\bar{\mathbf{I}}$ is a block identity matrix which is non-zero only between the pth and $(p+l)$th

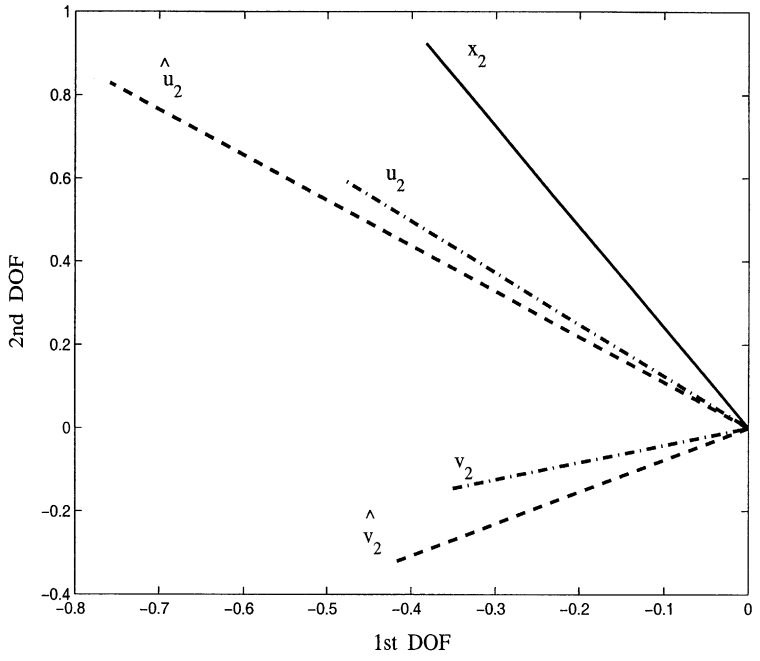

Fig. 3. Graphical (vector) representation of the real and imaginary parts of the second complex mode: 'O' origin; '–' normal mode $\mathbf{x}_2$; '- -' real and imaginary parts of the complex mode $\hat{\mathbf{z}}_2$ normalised using Eq. (2.4) with $\theta_2 = 2s_2$; '-.-' real and imaginary parts of the optimally normalised complex mode $\mathbf{z}_2$ obtained from Eq. (4.21).

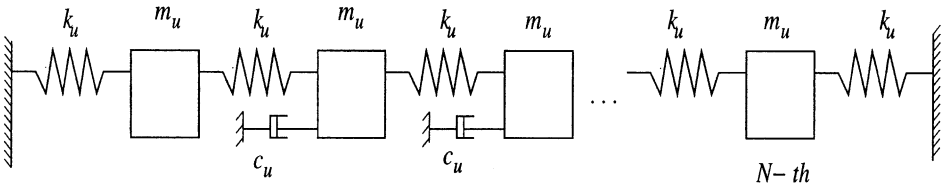

Fig. 4. Linear array of N spring–mass oscillators: $N = 10$, $m_u = 1$ kg, $k_u = 10$ N/m and $c_u = 0.5$ N m/s.

entries along the diagonal, so that 'p' denotes the first damped mass and $(p + l)$ the last one. For the numerical calculations, we have considered a 10-dof system so that $N = 10$. Values of the mass and stiffness associated with each unit are assumed to be the same with numerical values of $m_u = 1$ kg, $k_u = 10$ N/m. The start and end positions of the dampers are assumed to be $p = 6$ and $(p + l) = 9$ with values for each unit of $c_u = 0.5$ N m/s. Complex eigenvalues and Q-factors of the system are shown in Table 1. Low values of Q-factor indicate that the damping is quite high.

Optimal complex modes of the system are obtained using Eq. (4.21). Since all the modes are complex, synchronous motion, as in the case of classical modes, does not exist. This causes difficulty for graphical representation of complex modes [29]. Luo [30] has presented a method to describe complex modes using spirals where each spiral represents motion of a coordinate on the complex plane. Although this representation has complete information, it is difficult to visualise the nature of the motion physically. Another approach, due to [29,31], uses a collection of

Table 1
Complex eigenvalues and Q factors of the 10-dof system

Mode number	Complex eigenvalues	Q-factors
1	-0.1237 ± 0.9001i	3.6370
2	-0.1099 ± 1.7657i	8.0301
3	-0.0994 ± 2.6299i	13.2294
4	-0.0872 ± 3.4137i	19.5708
5	-0.0805 ± 4.1456i	25.7536
6	-0.0801 ± 4.7737i	29.8135
7	-0.0878 ± 5.3270i	30.3362
8	-0.0987 ± 5.7416i	29.0932
9	-0.0874 ± 6.1500i	35.2034
10	-0.1453 ± 6.1671i	21.1986

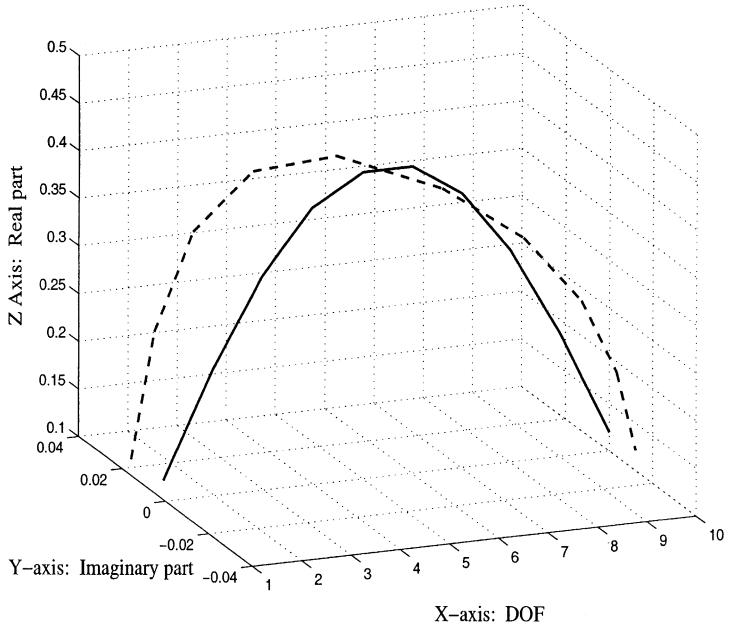

Fig. 5. Graphical representation of the optimal complex mode shape and the normal mode shape for first mode: '–' normal mode; '- -' optimal complex mode.

successive configurations (snap-shots) during motion at various instances of time over one period. This approach, although physically more appealing, requires many diagrams (ideally infinitely many) to represent even a single complex mode.

In this paper, we have tried to represent each complex mode in a single diagram similar to what we can do with normal modes. Optimal complex modes are used for plotting because they are closest to their corresponding normal modes. Fig. 5 shows such a plot for the first mode.

A three-dimensional (3-D) diagram is used where the X-axis denotes the dof and the real and imaginary parts are plotted along Z and Y axes, respectively.

Fig. 6 shows the projection of Fig. 5 in the XZ-plane. Observe that the real part of the optimal complex mode is close to the corresponding normal mode. Projection of Fig. 5 in the XY-plane is shown in Fig. 7. The normal mode appears as a straight line because it exists only in the XZ-plane at $y = 0$. Interestingly, observe that the imaginary part of the optimal complex mode has a shape similar to the second normal mode.

Fig. 8 shows the second optimal complex mode and second normal mode. Fig. 9 shows the projection of this figure in the XZ-plane. Observe that the real part of the optimal complex mode is close to the corresponding normal mode. Projection of Fig. 8 in the XY-plane is shown in Fig. 10. Note that the imaginary part of the optimal complex mode has a shape similar to the first normal mode.

Similar diagrams can also be plotted for other modes (not shown here). In all cases, we observe that the real parts of the optimal complex modes are very close to their corresponding undamped modes. However, the imaginary parts do not follow any such general trend. The approach presented to plot the complex modes is useful for exploring their nature. One can use commercial software (MATLAB^{TM} for example) to plot these 3-D diagrams and can 'rotate' them to learn more about their nature. However, one difficulty is that this approach cannot be extended to visualise modes of 2-D systems in a straightforward way.

The results shown here demonstrate that the optimal complex modes can provide good physical insight. It should be noted that any other (complex) normalisation procedure is likely to change

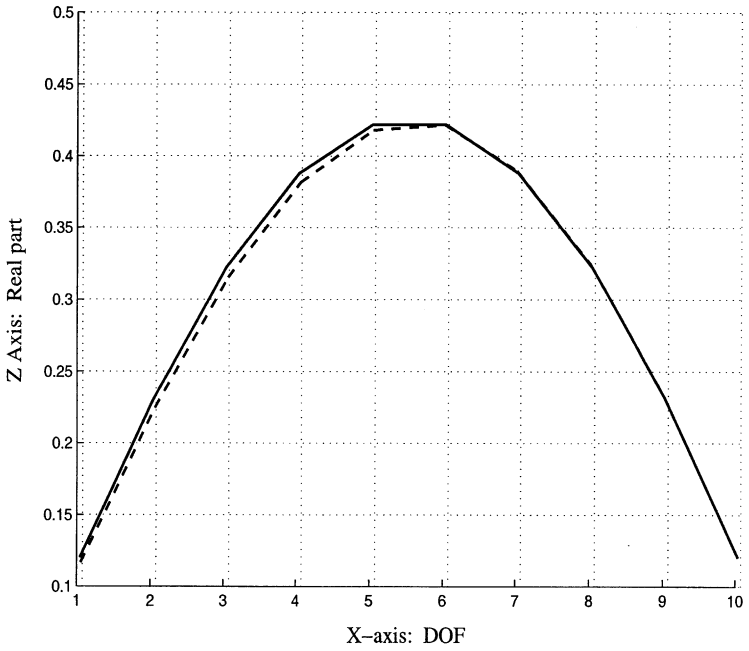

Fig. 6. Graphical representation of the optimal complex mode shape and the normal mode shape for first mode along XZ-plane: '–' normal mode; '- -' optimal complex mode.

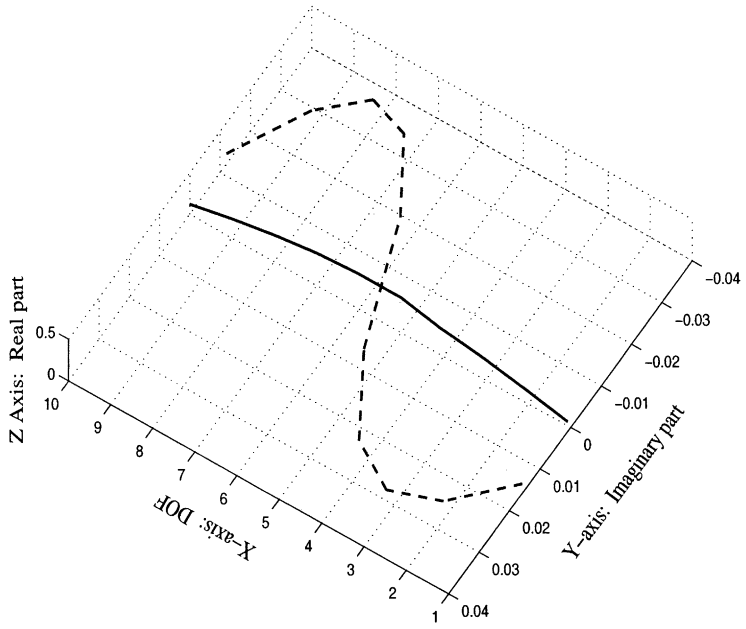

Fig. 7. Graphical representation of the optimal complex mode shape and the normal mode shape for first mode along XY-plane: '–' normal mode; '- -' optimal complex mode.

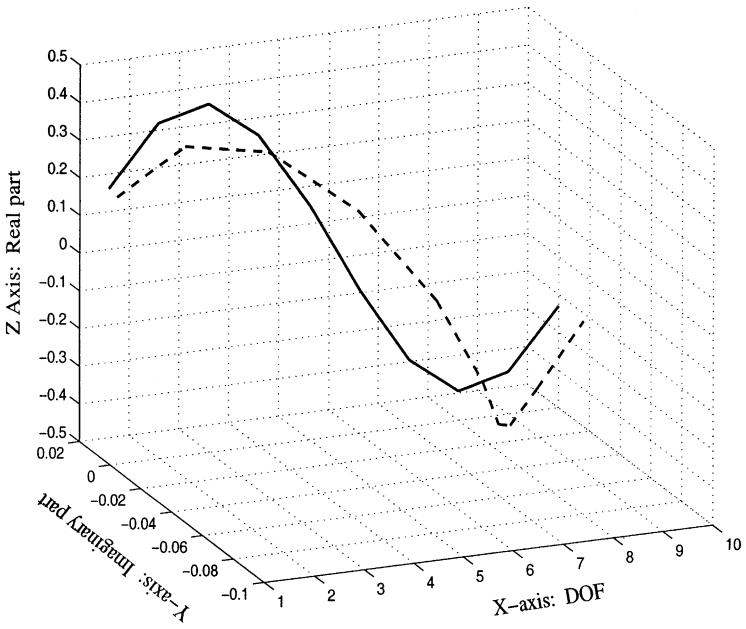

Fig. 8. Graphical representation of the optimal complex mode shape and the normal mode shape for second mode: '–' normal mode; '- -' optimal complex mode.

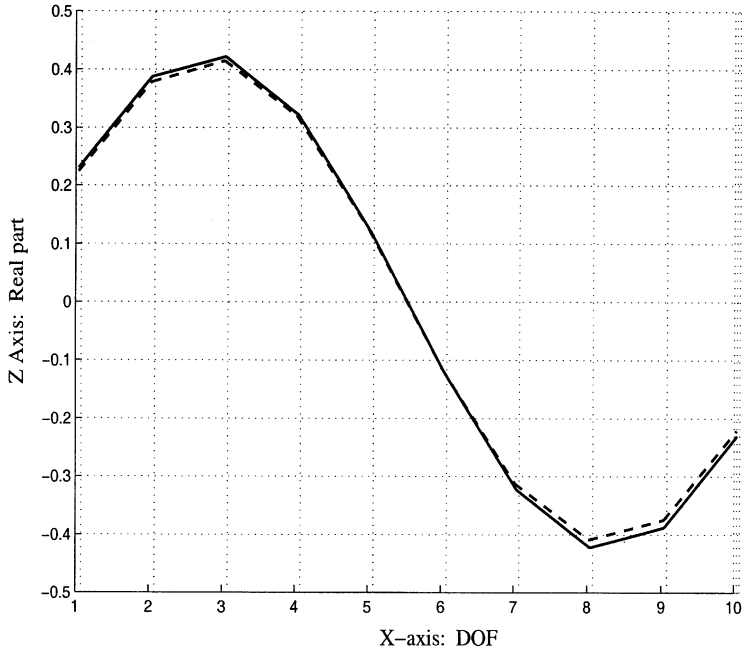

Fig. 9. Graphical representation of the optimal complex mode shape and the normal mode shape for second mode along XZ-plane: '–' normal mode; '- -' optimal complex mode.

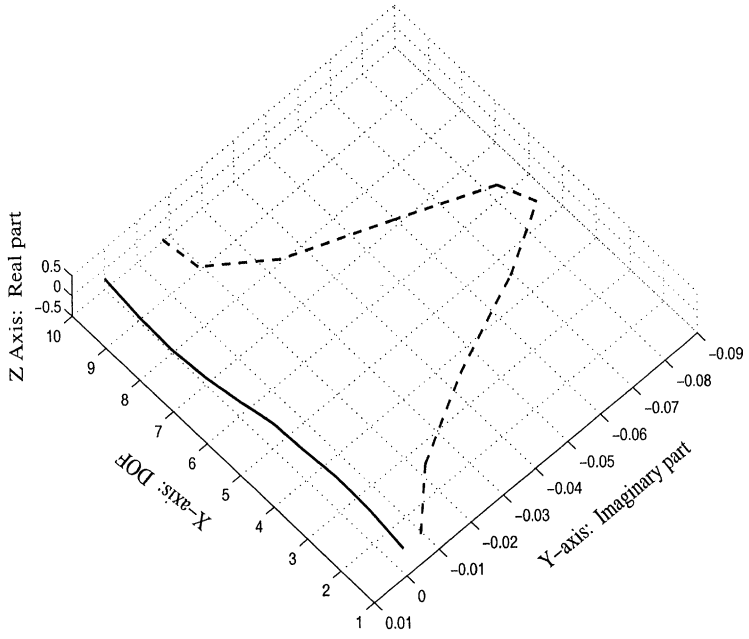

Fig. 10. Graphical representation of the optimal complex mode shape and the normal mode shape for second mode along XY-plane: '–' normal mode; '- -' optimal complex mode.

the 'shape' of the complex modes and consequently it may not be possible to visualise them like the normal modes (see the example in Section 6.2). The answer to the question, how close are the optimal complex modes to their corresponding normal modes, lies in how much 'non-proportionality' there is in the damping. This issue is addressed in the next section.

5. An index of non-proportionality

5.1. Theory

In order to quantify the extent of non-proportionality, different authors have proposed different types of measure. Imregun and Ewins [3] have proposed *modal complexity factors* based on the phase and amplitude of the elements of a complex modal vector. Many authors have proposed *non-proportionality indices*. These indices can be broadly divided into two types: (a) those using system property matrices, and (b) those using only complex modes.

In the first category, an index based on driving frequency and elements of the modal damping matrix is given in [10]. Bhaskar [32] has proposed a non-proportionality index based on the error introduced by ignoring the coupling terms in the modal damping matrix. Tong et al. [33] developed an analytical index based on the minimum and maximum of the eigenvalues of the modal damping matrix for quantification of the non-proportionality for discrete vibrating systems. Based on Tong et al. [33] and Shahruz [34], it may be concluded that a suitable index for non-proportionality should include the damping matrix and natural frequencies as well as the excitation vector.

Parter and Sing [35] and Nair and Sing [36] have developed several indices based on modal phase difference, modal polygon areas, relative magnitude of coupling terms in the modal damping matrix, system response, Nyquist plot, etc. Later, based on the idea related to the modal polygon area and by minimisation of the squared norm of the imaginary part of complex modes, two more indices of non-proportionality were proposed in [29]. Prells and Friswell [37] have shown that the (complex) modal matrix of a non-proportionally damped system depends on an orthonormal matrix, which represents the phase between different dof's of the system. For proportionally damped systems, this matrix becomes an identity matrix and consequently they have used this orthonormal matrix as an indicator of non-proportionality. Recently, Liu et al. [38] proposed three indices to measure the damping non-proportionality. The first index measures the correlation between the real and imaginary parts of the complex modes, the second index measures the magnitude of the imaginary parts of the complex modes and the third index quantifies the degree of modal coupling. These indices are based on the fact that the complex modal matrix can be decomposed into a product of a real and a complex matrix.

Here, an index of non-proportionality is developed based on the optimal complex modes discussed in the last section. Because the optimal complex mode $\mathbf{z}_k$ is closest to the normal mode $\mathbf{x}_k$, the difference between them naturally gives a measure of non-proportionality. For each mode, we define the index of non-proportionality as

$$I_k = \frac{||\mathbf{z}_k - \mathbf{x}_k||}{||\mathbf{x}_k||} \tag{5.1}$$

where the optimal complex mode $\mathbf{z}_k$ is defined in Eq. (4.21). Using this expression, the index of non-proportionality can be expressed as

$$I_k = \left|\left| \frac{\hat{\mathbf{u}}_k(\hat{\mathbf{u}}_k^T\mathbf{x}_k) + \hat{\mathbf{v}}_k(\hat{\mathbf{v}}_k^T\mathbf{x}_k)}{\|\hat{\mathbf{u}}_k\|^2 + \|\hat{\mathbf{v}}_k\|^2} - \mathbf{x}_k + \mathrm{i}\,\frac{\hat{\mathbf{v}}_k(\hat{\mathbf{u}}_k^T\mathbf{x}_k) - \hat{\mathbf{u}}_k(\hat{\mathbf{v}}_k^T\mathbf{x}_k)}{\|\hat{\mathbf{u}}_k\|^2 + \|\hat{\mathbf{v}}_k\|^2} \right|\right| \Big/ \|\mathbf{x}_k\|. \tag{5.2}$$

Note that in order to apply this index, the knowledge of the system property matrices is not required but we do need to know the normal modes of the system. The normal modes can be obtained, either from a FE model, or from experiments [39–41]. The index of non-proportionality defined in Eq. (5.1) is in general different for different modes. To obtain an overall measure of the non-proportionality of damping, the mean and the standard deviation of I_k, $\forall k = 1, \ldots, n$, given by

$$\mathscr{M} = \frac{\sum_{k=1}^{n} I_k}{n} \tag{5.3}$$

and

$$\mathscr{S} = \sqrt{\frac{1}{n-1}\sum_{k=1}^{n} (I_k - \mathscr{M}^2)}. \tag{5.4}$$

may be used. The above two expressions are expected to provide a good indication of the non-proportionality of damping for systems with large dof's.

Because the system property matrices do not explicitly appear in Eq. (5.1), it can also be applied to non-viscously damped systems. However, Eq. (5.1) can be related with the system property matrices if explicit expressions for optimal complex modes are used. To show this, we consider a simple case, namely viscously damped systems with light damping. Assuming first-order perturbation, the complex modes can be approximately expressed as

$$\mathbf{z}_k \approx \mathbf{x}_k + \mathrm{i}\sum_{\substack{j=1 \\ j\neq k}}^{N} \frac{\omega_j C'_{jk}}{(\omega_k^2 - \omega_j^2)}\mathbf{x}_j. \tag{5.5}$$

In the above expressions, $C'_{jk} = \mathbf{x}_j^T\mathbf{C}\mathbf{x}_k$ are the elements of the damping matrix in modal coordinates. This result was obtained by Rayleigh [1] (see Section 102, Eq. (6)). It can be shown that this expression may also be regarded as the expression of optimally normalised complex modes up to first-order perturbation approximation. Now, using Eq. (5.1), the index of non-proportionality reads

$$I_k \approx \frac{\left|\left| \mathrm{i}\sum_{\substack{j=1 \\ j\neq k}}^{N} \frac{\omega_j C'_{jk}}{(\omega_k^2 - \omega_j^2)}\mathbf{x}_j \right|\right|}{\|\mathbf{x}_k\|} \leqslant \sum_{\substack{j=1 \\ j\neq k}}^{N} \left| \frac{\omega_j C'_{jk}}{(\omega_k^2 - \omega_j^2)} \right| \frac{\|\mathbf{x}_j\|}{\|\mathbf{x}_k\|}. \tag{5.6}$$

This simple analysis illustrates how the index of non-proportionality depends on the off-diagonal terms of the modal damping matrix and spacing between the natural frequencies, the two most important factors responsible for non-proportionality of damping.

Note that Eq. (5.1) can also be used as a measure of the difference between a complex mode (not necessarily optimally normalised) and the corresponding normal mode. It is expected that the

values of I_k obtained from Eq. (5.1) will be minimum if the complex modes are optimally normalised, that is, when Eq. (5.2) is used. Thus, for all other normalisation procedures, the values of I_k will be more than the non-proportionality index, which by definition uses optimal complex modes in Eq. (5.1). In Section 6.2, these facts will be illustrated numerically using other normalisation methods.

5.2. Numerical examples

5.2.1. A 30-dof system

A system consisting of a linear array of spring–mass oscillators and dampers, similar to the one shown in Fig. 4, except, with $N = 30$ is considered. The same numerical values considered in Section 4.2.2 are assumed for all the system parameters. The position of damping is also assumed to be the same. The indices of non-proportionality obtained from Eq. (5.2) are shown in Fig. 11 for all 30 modes. Mean and standard deviation of the non-proportionality index, obtained from Eqs. (5.3) and (5.4), are shown in this figure. These results show how the proposed approach based on mean and standard deviation of the non-proportionality index gives an estimate of overall non-proportionality of the system.

5.2.2. A four-dof system with non-viscous damping

So far, the examples have considered viscously damped systems. In this section, we consider a non-viscously damped four-dof system whose equations of motion can be described by Eq. (3.1).

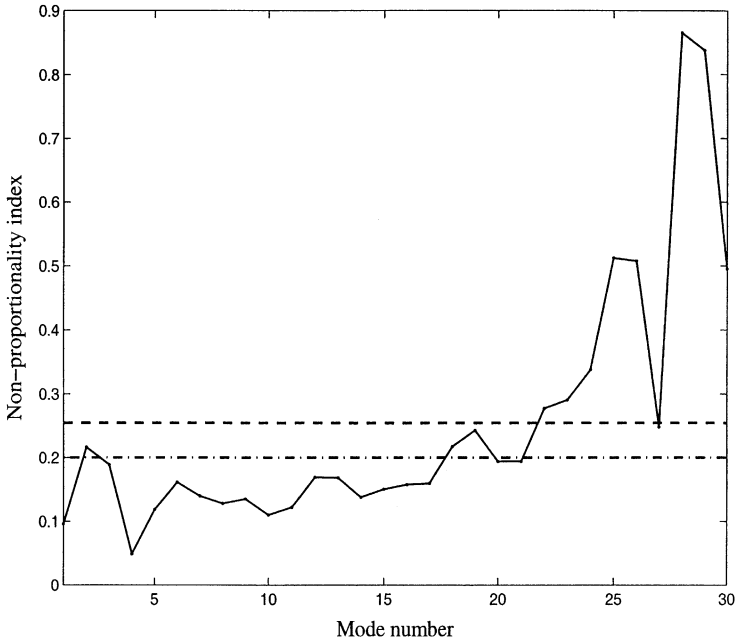

Fig. 11. The index of non-proportionality of the 30-dof system: '–' values at different modes; '- -' mean; '-.-' standard deviation.

The mass and stiffness matrices of the system are

$$\mathbf{M} = \mathrm{diag}[1, 2, 2, 1] \quad \text{and} \quad \mathbf{K} = \begin{bmatrix} 5 & -3 & 0 & 0 \\ -3 & 7 & -4 & 0 \\ 0 & -4 & 7 & -3 \\ 0 & 0 & -3 & 5 \end{bmatrix}. \tag{5.7}$$

These values are taken from Ref. [38]. The non- viscous damping model is assumed to be the GHM model (see [42] and references therein). The matrix of damping functions is assumed to be of the form

$$\mathscr{G}(t) = \mathbf{C}_v(\delta(t) + [\mu_1 e^{-\mu_1 t} + \mu_2 e^{-\mu_2 t}]); \quad \mu_1, \mu_2 > 0 \tag{5.8}$$

where the coefficient matrix

$$\mathbf{C}_v = \begin{bmatrix} C_{11} & 0 & 0 & 0 \\ 0 & 0.2 & 0 & 0 \\ 0 & 0 & 0.2 & 0 \\ 0 & 0 & 0 & 0.1 \end{bmatrix}. \tag{5.9}$$

The damping expressed in Eq. (5.8) is a linear combination of the viscous and non-viscous damping models. Taking the Laplace transform of Eq. (5.8) one obtains

$$\mathbf{G}(s) = \mathbf{C}_v + \left[\mathbf{C}_v \frac{(\mu_1 + \mu_2)s + 2\mu_1\mu_2}{s^2 + (\mu_1 + \mu_2)s + \mu_1\mu_2}\right]. \tag{5.10}$$

Using this expression and following the procedure outlined in Ref. [25], the elastic modes and the non-viscous modes of the system can be obtained. As mentioned before, only the (complex) elastic modes are effected by non-proportionality of the damping. Using the elastic modes, the index of non-proportionality can be obtained using Eq. (5.2). When $C_{11} = 0.1$, all the relationships in Eq. (1.4) are satisfied and consequently we say that the non-viscously damped system is proportionally damped. Fig. 12 shows the non-proportionality index (the solid line) for values of C_{11} ranging from 0.1 to 1.0. For comparing the results with the viscously damped system, in the same figure the index value is plotted (the dashed line) by neglecting the second part of Eq. (5.10). The general trend of the non-proportionality index for the viscously and non-viscously damped system is quite similar for the first and second modes while they are different for the third and fourth modes.

Note that, for all four modes, values of the non-proportionality index are zero when $C_{11} = 0.1$. This denotes that the damping is proportional for this value of C_{11} as expected. In contrast to the non-viscously damped system for all the modes of the viscously damped system, the index values increase with increasing values of C_{11}. Further, observe that the index of non-proportionality is more for modes 3 and 4 compared to those for modes 1 and 2. The reason for this can be traced back to the spacing between the natural frequencies. The undamped natural frequencies (in rad/s) of the system are, $\omega_1 = 0.7071$, $\omega_2 = 1.7647$, $\omega_3 = 2.4495$ and $\omega_4 = 2.7177$. Close values of ω_3 and ω_4 are clearly responsible for higher values of the non-proportionality index in these modes. Another fact emerging from these results is that when the system has closely spaced natural

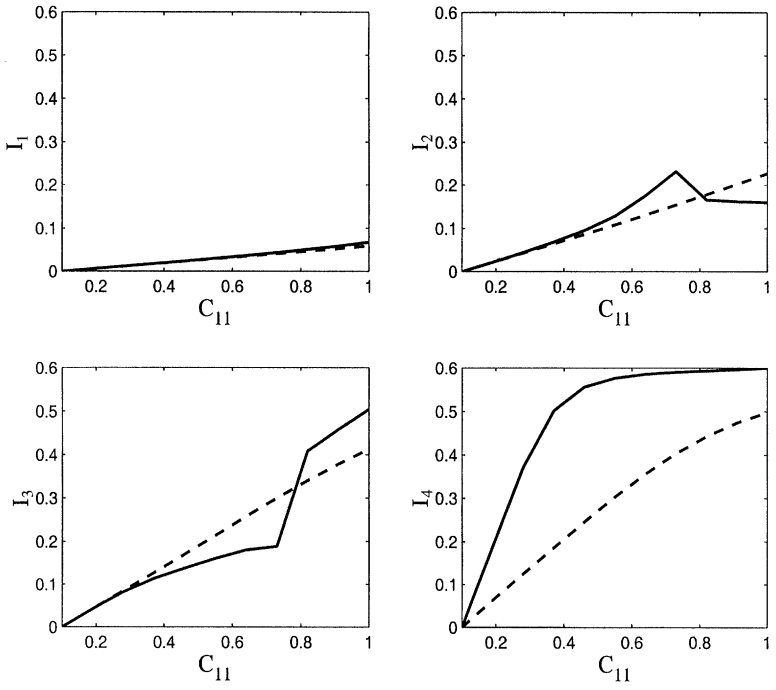

Fig. 12. The index of non-proportionality for the four modes: '–' non-viscously damped system; '- -' viscously damped system.

frequencies the non-proportionality index of viscously and non-viscously damped systems differs significantly.

6. Alternative normalisation methods

6.1. Theory

We define the merit function χ^2 as the weighted sum of χ_R^2 and χ_I^2, that is,

$$\chi^2 = \gamma_R \chi_R^2 + \gamma_I \chi_I^2 \tag{6.1}$$

where γ_R, $\gamma_I \in \mathbb{R}$ are the weights associated with χ_R^2 and χ_I^2, respectively. This general approach gives the flexibility to choose different weights associated with the real and the imaginary parts of complex modes. This approach might be useful in practice, for example, in the context of experimental modal identification, often, the imaginary parts are comparatively more erroneous than the real parts and one may wish to give less weighting to the imaginary parts compared to the real parts while determining optimal complex modes. The merit function in Eq. (4.18) is a special case of Eq. (6.1) when $\gamma_R = \gamma_I$. Note that χ^2 in Eq. (4.18) can also be obtained directly by using l_2 norm in $\mathbb{C}^N$ as $\chi^2 = \sum_{j=1}^{n} \varepsilon_j^{*T} \varepsilon_j$. The analytical treatment in Section 4.1 is adopted in view of extending it to this general case being discussed here.

Now, using χ^2 in Eq. (6.1), Eqs. (4.14)–(4.17) can be combined into two equations and may be expressed in a matrix form as

$$\begin{bmatrix} \gamma_R(\hat{\mathbf{u}}_k^T\hat{\mathbf{u}}_k)+\gamma_I(\hat{\mathbf{v}}_k^T\hat{\mathbf{v}}_k) & (-\gamma_R+\gamma_I)(\hat{\mathbf{u}}_k^T\hat{\mathbf{v}}_k) \\ (-\gamma_R+\gamma_I)(\hat{\mathbf{u}}_k^T\hat{\mathbf{v}}_k) & \gamma_R(\hat{\mathbf{v}}_k^T\hat{\mathbf{v}}_k)+\gamma_I(\hat{\mathbf{u}}_k^T\hat{\mathbf{u}}_k) \end{bmatrix} \begin{Bmatrix} \alpha_k \\ \beta_k \end{Bmatrix} = \begin{Bmatrix} \gamma_R(\hat{\mathbf{u}}_k^T\mathbf{x}_k) \\ -\gamma_R(\hat{\mathbf{v}}_k^T\mathbf{x}_k) \end{Bmatrix}. \tag{6.2}$$

Values of α_k and β_k have to be determined by solving this equation. Assume

$$\gamma_I = \eta\gamma_R \tag{6.3}$$

for some $\eta \in \mathbb{R}$. Using this, Eq. (6.2) can be rewritten as

$$[\mathbf{D}_k - \mathbf{Q}_k]\begin{Bmatrix} \alpha_k \\ \beta_k \end{Bmatrix} = \begin{Bmatrix} \hat{\mathbf{u}}_k^T\mathbf{x}_k \\ -\hat{\mathbf{v}}_k^T\mathbf{x}_k \end{Bmatrix} \tag{6.4}$$

where

$$\mathbf{D}_k = \begin{bmatrix} (\hat{\mathbf{u}}_k^T\hat{\mathbf{u}}_k)+\eta(\hat{\mathbf{v}}_k^T\hat{\mathbf{v}}_k) & 0 \\ 0 & (\hat{\mathbf{v}}_k^T\hat{\mathbf{v}}_k)+\eta(\hat{\mathbf{u}}_k^T\hat{\mathbf{u}}_k) \end{bmatrix} \tag{6.5}$$

and

$$\mathbf{Q}_k = \begin{bmatrix} 0 & (1-\eta) \\ (1-\eta) & 0 \end{bmatrix}(\hat{\mathbf{u}}_k^T\hat{\mathbf{v}}_k). \tag{6.6}$$

The constants α_k and β_k should be obtained from Eq. (6.4) by inverting the associated coefficient matrix as

$$\begin{aligned} \begin{Bmatrix} \alpha_k \\ \beta_k \end{Bmatrix} &= [\mathbf{D}_k - \mathbf{Q}_k]^{-1}\begin{Bmatrix} \hat{\mathbf{u}}_k^T\mathbf{x}_k \\ -\hat{\mathbf{v}}_k^T\mathbf{x}_k \end{Bmatrix} = [\mathbf{I} - \mathbf{D}_k^{-1}\mathbf{Q}_k]^{-1}\mathbf{D}_k^{-1}\begin{Bmatrix} \hat{\mathbf{u}}_k^T\mathbf{x}_k \\ -\hat{\mathbf{v}}_k^T\mathbf{x}_k \end{Bmatrix} \\ &= [\mathbf{I} - \mathbf{R}_k]^{-1}\left(\mathbf{D}_k^{-1}\begin{Bmatrix} \hat{\mathbf{u}}_k^T\mathbf{x}_k \\ -\hat{\mathbf{v}}_k^T\mathbf{x}_k \end{Bmatrix}\right) \end{aligned} \tag{6.7}$$

where

$$\mathbf{R}_k = \mathbf{D}_k^{-1}\mathbf{Q}_k = (1-\eta)\begin{bmatrix} 0 & r_{1_k} \\ r_{2_k} & 0 \end{bmatrix} \tag{6.8}$$

with

$$\begin{aligned} r_{1_k} &= \frac{\hat{\mathbf{u}}_k^T\hat{\mathbf{v}}_k}{\|\hat{\mathbf{u}}_k\|^2 + \eta\|\hat{\mathbf{v}}_k\|^2} \\ r_{2_k} &= \frac{\hat{\mathbf{u}}_k^T\hat{\mathbf{v}}_k}{\eta\|\hat{\mathbf{u}}_k\|^2 + \|\hat{\mathbf{v}}_k\|^2}. \end{aligned} \tag{6.9}$$

Denote

$$\left\{ \begin{array}{c} \alpha_{0_k} \\ \beta_{0_k} \end{array} \right\} = \mathbf{D}_k^{-1} \left\{ \begin{array}{c} \hat{\mathbf{u}}_k^T \mathbf{x}_k \\ -\hat{\mathbf{v}}_k^T \mathbf{x}_k \end{array} \right\} = \left\{ \begin{array}{c} \dfrac{\hat{\mathbf{u}}_k^T \mathbf{x}_k}{\|\hat{\mathbf{u}}_k\|^2 + \eta \|\hat{\mathbf{v}}_k\|^2} \\ -\dfrac{\hat{\mathbf{v}}_k^T \mathbf{x}_k}{\eta \|\hat{\mathbf{u}}_k\|^2 + \|\hat{\mathbf{v}}_k\|^2} \end{array} \right\}. \tag{6.10}$$

From Eq. (6.8), one obtains

$$\mathbf{R}_k^2 = (1-\eta)^2 \begin{bmatrix} r_{1_k} r_{2_k} & 0 \\ 0 & r_{2_k} r_{1_k} \end{bmatrix} = r_{1_k} r_{2_k} (1-\eta)^2 \mathbf{I}. \tag{6.11}$$

We also have the following identity:

$$[\mathbf{I} - \mathbf{R}_k][\mathbf{I} + \mathbf{R}_k] = [\mathbf{I} - \mathbf{R}_k^2]$$

or

$$[\mathbf{I} - \mathbf{R}_k]^{-1} = [\mathbf{I} + \mathbf{R}_k][\mathbf{I} - \mathbf{R}_k^2]^{-1}. \tag{6.12}$$

From Eq. (6.11),

$$[\mathbf{I} - \mathbf{R}_k^2] = (1 - r_{1_k} r_{2_k} (1-\eta)^2)\mathbf{I}$$

or

$$[\mathbf{I} - \mathbf{R}_k^2]^{-1} = \frac{1}{1 - r_{1_k} r_{2_k} (1-\eta)^2} \mathbf{I}. \tag{6.13}$$

So from Eq. (6.12),

$$[\mathbf{I} - \mathbf{R}_k]^{-1} = \frac{1}{1 - r_{1_k} r_{2_k} (1-\eta)^2} [\mathbf{I} + \mathbf{R}_k]. \tag{6.14}$$

Finally, using Eqs. (6.10) and (6.14), from Eq. (6.7) we obtain

$$\left\{ \begin{array}{c} \alpha_k \\ \beta_k \end{array} \right\} = \frac{1}{1 - r_{1_k} r_{2_k} (1-\eta)^2} [\mathbf{I} + \mathbf{R}_k] \left\{ \begin{array}{c} \alpha_{0_k} \\ \beta_{0_k} \end{array} \right\}. \tag{6.15}$$

Observe that the above expression reduces to the expressions of α_k and β_k obtained in Eq. (4.20) when $\eta = 1$. In principle, any value of η can be selected. The following two limiting cases may of interest:

Case 1: $\gamma_I = 0$, i.e. $\eta = 0$. In this case, the imaginary parts are ignored and only the sum of squares of the real parts are minimised. In this case, α_k and β_k need to satisfy Eqs. (4.14) and (4.15) only, which can be obtained directly from Eq. (6.15) by substituting $\eta = 0$. The result is

$$\alpha_k = \frac{(\hat{\mathbf{v}}_k^T \hat{\mathbf{v}}_k)(\hat{\mathbf{u}}_k^T \mathbf{x}_k) - (\hat{\mathbf{u}}_k^T \hat{\mathbf{v}}_k)(\hat{\mathbf{v}}_k^T \mathbf{x}_k)}{\|\hat{\mathbf{u}}_k\|^2 \|\hat{\mathbf{v}}_k\|^2 - \hat{\mathbf{u}}_k^T \hat{\mathbf{v}}_k}$$

and

$$\beta_k = \frac{(\hat{\mathbf{u}}_k^T \hat{\mathbf{v}}_k)(\hat{\mathbf{u}}_k^T \mathbf{x}_k) - (\hat{\mathbf{u}}_k^T \hat{\mathbf{u}}_k)(\hat{\mathbf{v}}_k^T \mathbf{x}_k)}{\|\hat{\mathbf{u}}_k\|^2 \|\hat{\mathbf{v}}_k\|^2 - \hat{\mathbf{u}}_k^T \hat{\mathbf{v}}_k}. \tag{6.16}$$

The optimal complex mode $\mathbf{z}_k$ can be obtained by substituting these values in Eq. (4.5). It is expected that only the real parts of complex modes will be closest to their corresponding normal modes.

Case 2: $\gamma_R = 0$, i.e. $\eta = \infty$. In this case, the real parts are not considered and only the sum of squares of the imaginary parts are minimised. This normalisation was considered by Bhaskar [29]. In this case, α_k and β_k need to satisfy Eqs. (4.16) and (4.17) only. From these equations observe that a unique solution cannot be obtained. However, from Eqs. (4.16) and (4.17) one can obtain the following ratios, respectively:

$$\frac{\beta_k}{\alpha_k} = -\frac{||\hat{\mathbf{v}}_k||^2}{\hat{\mathbf{u}}_k^T \hat{\mathbf{v}}_k} \tag{6.17}$$

and

$$\frac{\beta_k}{\alpha_k} = -\frac{\hat{\mathbf{u}}_k^T \hat{\mathbf{v}}_k}{||\hat{\mathbf{u}}_k||^2}. \tag{6.18}$$

Using these values, from Eq. (4.5) the optimal complex mode can be expressed as

$$\mathbf{z}_k = \left\{ \left(\hat{\mathbf{u}}_k + \hat{\mathbf{v}}_k \frac{||\hat{\mathbf{v}}_k||^2}{\hat{\mathbf{u}}_k^T \hat{\mathbf{v}}_k} \right) + \mathrm{i} \left(\hat{\mathbf{v}}_k - \hat{\mathbf{u}}_k \frac{||\hat{\mathbf{v}}_k||^2}{\hat{\mathbf{u}}_k^T \hat{\mathbf{v}}_k} \right) \right\} \alpha_k \tag{6.19}$$

or

$$\mathbf{z}_k = \left\{ \left(\hat{\mathbf{u}}_k + \hat{\mathbf{v}}_k \frac{\hat{\mathbf{u}}_k^T \hat{\mathbf{v}}_k}{||\hat{\mathbf{u}}_k||^2} \right) + \mathrm{i} \left(\hat{\mathbf{v}}_k - \hat{\mathbf{u}}_k \frac{\hat{\mathbf{u}}_k^T \hat{\mathbf{v}}_k}{||\hat{\mathbf{u}}_k||^2} \right) \right\} \alpha_k \tag{6.20}$$

where α_k is an arbitrary real scalar. However, note that the relative phase of each complex mode is being fixed by this normalisation approach.

6.2. Numerical example

We again consider the two-dof examples taken in Section 4.2.1. Here the intention is to compare complex modes and the associated indices of non-proportionality obtained from different normalisation procedures. Recall that the non-proportionality index defined by Eq. (5.1) is itself a measure of the difference between a complex mode and the corresponding normal mode. The normalisation methods considered here are:

(a) $\theta_k = 2s_k$ in Eq. (2.4) as given by Eq. (2.5a),
(b) $\theta_k = 2\mathrm{i}\Im(s_k)$ in Eq. (2.4) as given in Eq. (2.5b),
(c) $\theta_k = 1$ in Eq. (2.4) as given by Eq. (2.5c),
(d) $\eta = 0$, that is case 1 in the previous subsection,
(e) finally the optimally normalised complex modes as proposed in Section 4.1.

The results are summarised in Table 2. The undamped modes given by Eq. (4.22) are also shown in the table for the purpose of comparison and the indices of non-proportionality for the two modes are denoted by I_1 and I_2. Note that normalization methods (a) and (b) produce very close results. This is expected because the real parts of the eigenvalues are much smaller compared to the imaginary parts. It was mentioned before that the complex modes obtained using normalisation method (c) is inconsistent with the unity mass normalised undamped modes. This fact can be easily verified by looking at the complex modes corresponding to case (c) in Table 2. Observe that non-proportionality indices have the highest values for this case,

Table 2
Complex modes and indices of non-proportionality for different normalisation procedures

Normalisation method	Mode 1	Mode 2
Undamped modes	$\mathbf{x}_1 = \begin{Bmatrix} 0.9239 \\ 0.3827 \end{Bmatrix}$	$\mathbf{x}_2 = \begin{Bmatrix} -0.3827 \\ 0.9239 \end{Bmatrix}$
(a)	$\mathbf{z}_1 = \begin{Bmatrix} 0.8463 - 0.3349\mathrm{i} \\ 0.7538 + 0.3877\mathrm{i} \end{Bmatrix}$ $I_1 = 0.6374$	$\mathbf{z}_2 = \begin{Bmatrix} -0.7589 - 0.4241\mathrm{i} \\ 0.8296 - 0.3259\mathrm{i} \end{Bmatrix}$ $I_2 = 0.6607$
(b)	$\mathbf{z}_1 = \begin{Bmatrix} 0.8386 - 0.3526\mathrm{i} \\ 0.7615 + 0.3715\mathrm{i} \end{Bmatrix}$ $I_1 = 0.6427$	$\mathbf{z}_2 = \begin{Bmatrix} -0.7736 - 0.3936\mathrm{i} \\ 0.8150 - 0.3574\mathrm{i} \end{Bmatrix}$ $I_2 = 0.6689$
(c)	$\mathbf{z}_1 = \begin{Bmatrix} 0.0426 - 0.1043\mathrm{i} \\ 0.0992 - 0.0342\mathrm{i} \end{Bmatrix}$ $I_1 = 0.9323$	$\mathbf{z}_2 = \begin{Bmatrix} -0.1008 + 0.0328\mathrm{i} \\ 0.0395 - 0.1012\mathrm{i} \end{Bmatrix}$ $I_2 = 0.9343$
(d)	$\mathbf{z}_1 = \begin{Bmatrix} 0.9239 + 0.2625\mathrm{i} \\ 0.3827 + 0.8085\mathrm{i} \end{Bmatrix}$ $I_1 = 0.8500$	$\mathbf{z}_2 = \begin{Bmatrix} -0.3827 - 0.8515\mathrm{i} \\ 0.9239 + 0.2502\mathrm{i} \end{Bmatrix}$ $I_2 = 0.8875$
(e)	$\mathbf{z}_1 = \begin{Bmatrix} 0.6205 - 0.1436\mathrm{i} \\ 0.4812 + 0.3467\mathrm{i} \end{Bmatrix}$ $I_1 = 0.4926$	$\mathbf{z}_2 = \begin{Bmatrix} -0.4794 - 0.3571\mathrm{i} \\ 0.5948 - 0.1479\mathrm{i} \end{Bmatrix}$ $I_2 = 0.5168$

indicating that these complex modes are the 'farthest' from the corresponding mass normalised undamped modes. Normalisation method (d) produces an interesting result. The real parts of complex modes turned out to be exactly the same as the corresponding undamped modes. However, because the imaginary parts of complex modes are neglected in case (d) they are not minimised. The higher values of non-proportionality indices indicate that these modes are actually not the closest to the undamped modes although the real parts are exactly the same as the undamped modes.

Now we turn our attention to the optimally normalised complex modes, that is, normalisation method (e). Note that the non-proportionality indices have the lowest values for this case. This shows that the optimal complex modes are the nearest to the undamped modes. To reconfirm this conclusion, the index of non-proportionality obtained for different values of η are shown in Fig. 13. It is clear that for both the modes the non-proportionality indices have the lowest values corresponding to $\eta = 1$, that is, when the optimal complex modes proposed in Section 4.1 are used.

7. Conclusions

When the damping is non-proportional, both viscously and non-viscously damped linear systems possess complex modes instead of classical normal modes. The presence of complex

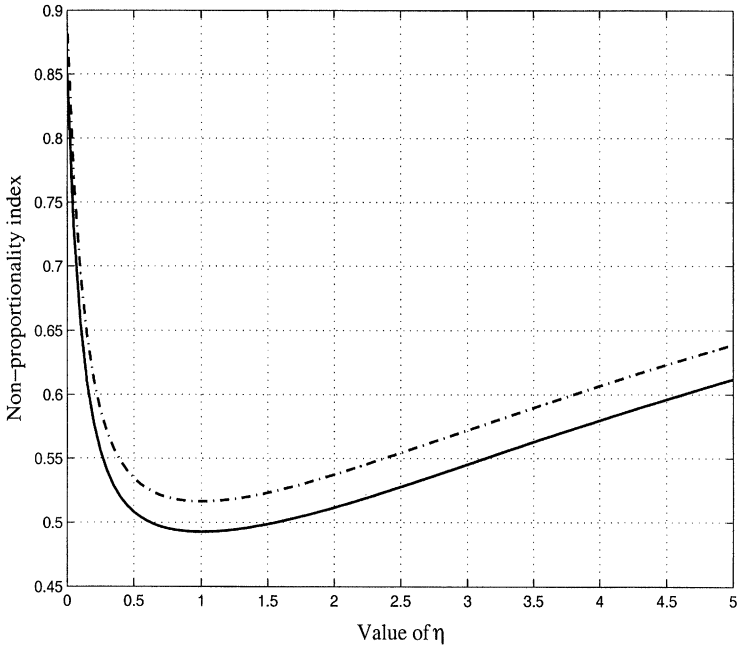

Fig. 13. The index of non-proportionality of the 2-dof system: '–' first mode; '-.-' second mode.

modes significantly complicates the analysis because, unlike normal modes' shapes, their 'shapes' are difficult to visualise. To solve this problem, a linear least-square method was presented to normalise the experimentally identified complex modes such that they become closest to their corresponding normal modes. Such complex modes were called *optimal complex modes*. Neither the damping matrix, nor the mass and stiffness matrices are required for optimal normalisation of complex modes. This fact makes this method very useful for practical purposes. It was observed that, even for systems with moderately high damping, the real parts of optimal complex modes are close to their corresponding normal modes. However, such a general conclusion for the imaginary parts of the optimal complex modes could not be drawn.

An index of non-proportionality, based on the difference between the optimal complex modes and their corresponding normal modes, was proposed. It was shown that this index can also be applied to non-viscously damped systems. In general, values of the proposed index of non-proportionality are different for different modes. To obtain an overall measure of the damping non-proportionality, use of the mean and the standard deviation of the index was suggested. This approach is likely to be useful for systems with large degrees of freedom.

Acknowledgements

The author is indebted to James Talbot for his careful reading of the manuscript. Financial support provided by the Nehru Memorial Trust, London, and the Cambridge Commonwealth Trust is greatly acknowledged.

Appendix A. Nomenclature

$\mathbf{C}$	viscous damping matrix
$\mathbf{C}'$	damping matrix in the modal coordinates
$\mathbf{G}(s)$	damping function in the Laplace domain
$\mathscr{G}(t)$	damping function in the time domain
I_j	non-proportionality index for jth mode
i	unit imaginary number, $\mathrm{i} = \sqrt{-1}$
$\mathbf{K}$	stiffness matrix
$\mathbf{M}$	mass matrix
$\mathscr{M}$	mean of non-proportionality index over all modes
m	order of the characteristic polynomial
N	degrees of freedom of the system
n	number of measured modes
p	number of non-viscous modes
Q_j	Q-factor for jth mode
$\mathbf{q}(t)$	vector of generalised coordinates
$\mathscr{S}$	standard deviation of non-proportionality index over all modes
s	Laplace domain parameter
s_j	jth eigenvalue of the system
t	time
$\mathbf{x}_j$	jth undamped mode
$\mathbf{X}$	matrix containing $\mathbf{x}_j$
$\mathbf{z}_j$	jth optimal complex mode
$\hat{\mathbf{z}}_j$	jth measured complex mode
$\hat{\mathbf{u}}_j$	real part of $\hat{\mathbf{z}}_j$
$\hat{\mathbf{v}}_j$	imaginary part of $\hat{\mathbf{z}}_j$
θ_j	theoretical normalisation constant for jth complex mode
λ_j	optimal normalisation constant associated with $\hat{\mathbf{z}}_j$
α_j	real part of λ_j
β_j	imaginary part of λ_j
ε_j	complex error vector associated with jth complex mode
ε_{R_j}	real part of ε_j
ε_{I_j}	imaginary part of ε_j
χ_R^2	objective function associated with ε_{R_j}
χ_I^2	objective function associated with ε_{I_j}
χ^2	combined objective function
γ_R	weight associated with χ_R^2
γ_I	weight associated with χ_I^2
η	relative weighting parameter, $\eta = \gamma_I/\gamma_R$
$\delta(t)$	Dirac delta function
μ_1, μ_2	parameters of the GHM damping model
ω_j	jth undamped natural frequency
$\mathbb{C}$	space of complex numbers

$\mathbb{R}$	space of real numbers
diag	a diagonal matrix
$\in$	belongs to
$\forall$	for all
det(•)	determinant of (•)
$\Re(\bullet)$	real part of (•)
$\Im(\bullet)$	imaginary part of (•)
$(\bullet)^T$	matrix transpose of (•)
$(\bullet)^*$	complex conjugation of (•)
$(\bullet)^{-1}$	matrix inverse of (•)
$(\dot{\bullet})$	derivative of (•) with respect to t
$\|\bullet\|$	l_2 norm of (•) in $\mathbb{R}^N$
$\|\bullet\|$	absolute value of (•)
dof	degree of freedom

References

[1] Lord Rayleigh, Theory of Sound, Vols. 1 and 2, 2nd edition, Dover Publications, New York, 1877, 1945 (Re-issue).
[2] T.K. Caughey, M.E.J. O'Kelly, Classical normal modes in damped linear dynamic systems, Transaction of ASME, Journal of Applied Mechanics 32 (1965) 583–588.
[3] M. Imregun, D.J. Ewins, Complex modes—origin and limits, Proceedings of the 13th International Modal Analysis Conference (IMAC), Nashville, TN, 1995, pp. 196–506.
[4] W.T. Thomson, C. Calkins, P. Caravani, A numerical study of damping, Earthquake Engineering and Structural Dynamics 3 (1974) 97–103.
[5] T.K. Hasselsman, Modal coupling in lightly damped structures, AIAA Journal 14 (1976) 1627–1628.
[6] D.L. Cronin, Approximation for determining harmonically excited response of non-classically damped systems, ASME Journal of Engineering for Industry 98 (1976) 43–47.
[7] R.W. Clough, S. Mojtahedi, Earthquake response analysis considering non-proportional damping, Earthquake Engineering and Structural Dynamics 4 (1976) 489–496.
[8] G.B. Warburton, S.R. Soni, Errors in response calculations for non-classically damped structures, Earthquake Engineering and Structural Dynamics 5 (1977) 365–376.
[9] S.M. Shahruz, F. Ma, Approximate decoupling of the equations of motion of linear underdamped system, Transaction of ASME, Journal of Applied Mechanics 55 (1988) 716–720.
[10] J. Bellos, D.J. Inman, Frequency response of non-proportionally damped, lumped parameter, linear systems, Transaction of ASME, Journal of Vibration and Acoustics 112 (1990) 194–201.
[11] S.M. Shahruz, Approximate decoupling of the equations of motion of damped linear systems, Journal of Sound and Vibration 136 (1990) 51–64.
[12] J.H. Hwang, F. Ma, On the approximate solution of non-classically damped linear systems, Transaction of ASME, Journal of Applied Mechanics 60 (1993) 695–701.
[13] I.W. Park, J.S. Kim, F. Ma, On the modal coupling in non-classically damped linear systems, Mechanics Research Communications 13 (1992) 407–413.
[14] S. Park, I.W. Park, F. Ma, Decoupling approximation of non-classically damped structures, AIAA Journal 30 (1992) 2348–2351.
[15] I.W. Park, J.S. Kim, F. Ma, Characteristics of modal coupling in non-classically damped systems under harmonic excitation, Transaction of ASME, Journal of Applied Mechanics 61 (1994) 77–83.
[16] S.M. Shahruz, P.A. Srimatsya, Approximate solutions of non-classically damped linear systems in normalized and physical coordinates, Journal of Sound and Vibration 201 (1997) 262–271.

[17] W. Gawronski, J.T. Sawicki, Response errors of non-proportionally lightly damped structures, Journal of Sound and Vibration 200 (1997) 543–550.
[18] M.A. Biot, Linear thermodynamics and the mechanics of solids, Proceedings of the Third US National Congress on Applied Mechanics, ASME, New York, 1958, pp. 1–18.
[19] S. Adhikari, Classical normal modes in non-viscously damped linear systems, AIAA Journal 39 (2001) 978–980.
[20] K.A. Foss, Coordinates which uncouple the equations of motion of damped linear dynamic systems, Transaction of ASME, Journal of Applied Mechanics 25 (1958) 361–364.
[21] D.E. Newland, On the modal analysis of nonconservative linear systems, Journal of Sound and Vibration 112 (1987) 69–96.
[22] A. Sestieri, R. Ibrahim, Analysis of errors and approximations in the use of modal coordinates, Journal of Sound and Vibration 177 (1994) 145–157.
[23] F.R. Vigneron, A natural modes model and modal identities for damped linear structures, Transaction of ASME, Journal of Applied Mechanics 53 (1986) 33–38.
[24] I. Fawzy, Orthogonality of generally normalized eigenvector and eigenrows, AIAA Journal 15 (1977) 276–278.
[25] S. Adhikari, Dynamics of non-viscously damped linear systems, ASCE Journal of Engineering Mechanics 128 (3) (2002) 328–339.
[26] D.R. Bland, Theory of Linear Viscoelasticity, Pergamon, London, 1960.
[27] A. Muravyov, Analytical solutions in the time domain for vibration problems of discrete viscoelastic systems, Journal of Sound and Vibration 199 (1997) 337–348.
[28] S. Adhikari, Eigenrelations for non-viscously damped systems, AIAA Journal 39 (8) (2001) 1624–1630.
[29] A. Bhaskar, Mode shapes during asynchronous motion and non-proportionality indices, Journal of Sound and Vibration 224 (1999) 1–16.
[30] D.Z. Luo, A graphic explanation of undamped and damped mode shapes and its application, Journal of Sound and Vibration 135 (1989) 351–356.
[31] D.E. Newland, Mechanical Vibration Analysis and Computation, Longman, Harlow and Wiley, New York, 1989.
[32] A. Bhaskar, Estimates of errors in the frequency response of non-classically damped system, Journal of Sound and Vibration 184 (1995) 59–72.
[33] M. Tong, Z. Liang, G.C. Lee, An index of damping non-proportionality for discrete vibrating systems, Journal of Sound and Vibration 174 (1994) 37–55.
[34] S.M. Shahruz, Comments on 'An index of damping non-proportionality for discrete vibrating systems', Journal of Sound and Vibration 186 (1995) 535–542.
[35] G. Parter, R. Sing, Quantification of the extent on non-proportional damping discrete vibratory systems, Journal of Sound and Vibration 104 (1986) 109–125.
[36] S.S. Nair, R. Sing, Examination of the validity of proportional damping approximations with two further numerical indices, Journal of Sound and Vibration 104 (1986) 348–350.
[37] U. Prells, M.I. Friswell, A measure of non-proportional damping, Mechanical Systems and Signal Processing 14 (2000) 125–137.
[38] K. Liu, M.R. Kujath, W. Zheng, Quantification of non-proportionality of damping in discrete vibratory systems, Computer and Structures 77 (2000) 557–569.
[39] S.R. Ibrahim, Computation of normal modes from identified complex modes, AIAA Journal 21 (1983) 446–451.
[40] S.Y. Chen, M.S. Ju, Y.G. Tsuei, Extraction of normal modes for highly coupled incomplete systems with general damping, Mechanical Systems and Signal Processing 10 (1996) 93–106.
[41] E. Balmès, New results on the identification of normal modes from experimental complex modes, Mechanical Systems and Signal Processing 11 (1997) 229–243.
[42] D.J. McTavis, P.C. Hughes, Modeling of linear viscoelastic space structures, Transaction of ASME, Journal of Vibration and Acoustics 115 (1993) 103–110.